Remote Sens. **2010**, *2*, 2607-2628; doi:10.3390/rs2112607

OPEN ACCESS

Remote Sensing

ISSN 2072-4292

www.mdpi.com/journal/remotesensing

Article

Hydraulic Geometry, GIS and Remote Sensing, Techniques against Rainfall-Runoff Models for Estimating Flood Magnitude in Ephemeral Fluvial Systems

Carmelo Conesa-Garcia [1,*], Vicente Caselles-Miralles [2], Juan M. Sanchez Tomas [2] and Rafael Garcia-Lorenzo [3]

[1] Department of Physical Geography, University of Murcia, Campus la Merced, s/n, 30001 Murcia, Spain

[2] Department of Physics of the Earth and Thermodynamics, University of Valencia, 46100 Burjassot, Spain; E-Mails: VicenteCaselles@uv.es (V.C.-M.); Juan.M.Sanchez@uv.es (J.M.S.T.)

[3] Autonomous Community of Murcia Region, Environmental Integration and Information Service, C/Catedrático Eugenio Ubeda, s/n, Murcia, Spain; E-Mail: rafaelgl@um.es

* Author to whom correspondence should be addressed; E-Mail: cconesa@um.es.

Received: 27 September 2010; in revised form: 3 November 2010 / Accepted: 10 November 2010 / Published: 23 November 2010

Abstract: This paper shows the combined use of remotely sensed data and hydraulic geometry methods as an alternative to rainfall-runoff models. Hydraulic geometric data and boolean images of water sheets obtained from satellite images after storm events were integrated in a Geographical Information System. Channel cross-sections were extracted from a high resolution Digital Terrain Model (DTM) and superimposed on the image cover to estimate the peak flow using HEC-RAS. The proposed methodology has been tested in ephemeral channels (*ramblas*) on the coastal zone in south-eastern Spain. These fluvial systems constitute an important natural hazard due to their high discharges and sediment loads. In particular, different areas affected by floods during the period 1997 to 2009 were delimited through HEC-GeoRAs from hydraulic geometry data and Landsat images of these floods (Landsat-TM5 and Landsat-ETM+7). Such an approach has been validated against rainfall-surface runoff models (SCS Dimensionless Unit Hydrograph, SCSD, Témez gamma HU Tγ and the Modified Rational method, MRM) comparing their results with flood hydrographs of the Automatic Hydrologic Information System (AHIS) in several ephemeral channels in the Murcia Region. The results obtained from the method providing a better fit were used to calculate different hydraulic geometry parameters, especially in residual flood areas.

Keywords: rainfall-runoff modeling; Geographic Information System (GIS); hydraulic geometry; remote sensing; flood hazard; ephemeral channels; Southeast Spain

1. Introduction

Hydraulic geometry methods commonly used for estimating flood peak discharges in ephemeral channels usually incorporate the dominant features of the channel shape in its formulae (width, *B*; depth, *d*; hydraulic radius, *R*; wet perimeter, *P*; slope, *S*) and its relations with the energy laws expressed in terms of flow. Ever since Lacey's classic equations [1,2] until the hydraulic geometry relationships and the Tinkler's critical flow regime [3], many proposals have been developed which, based on the regime theories, are adequate approaches for estimating flood discharges. In recent decades many attempts have been made to combine the remote sensing techniques with traditional channel geometry methods. In fact, Dingman and Sharma's regime equation [4] makes it possible to estimate the channel using geometric variables of the channel that are directly measurable in the field, and potentially measurable through satellite images, without having to deduce the bed roughness parameters, normally required for conventional hydraulic methods, such as the equations of Chezy or Manning. Another method for calculating the flow is by using satellite data based on the consideration of channel geometry at a given point together with the flow curves obtained by Leopold *et al*. [5] according to the depth and transversal area of the flow. The precision of the satellite observations, together with the *in situ* calibration and the use of high resolution DTMs in a GIS environment, have made it possible to construct new hydraulic models in this respect [6-8].

For semiarid areas, the flow geometry method is especially useful and has already been used by many authors as an indirect method for estimating flood discharges [9-12]. This method is based on the relations between channel hydraulic geometry and high flow conditions ('bankfull' and "flood-prone area"), and therefore constitutes an excellent instrument for predicting extreme hydrological events and the planning of areas at risk. The dry state of most of the channels in this area, and in south-eastern Spain in general, makes it easy to measure the geometric and roughness parameters needed to calculate peak flows in these systems which are barely instrumentalized. The satellite images provide valuable information about the surface covered by flood waters. Therefore, when this information is added to precise field data and high resolution terrain digital models, it could offer a more adequate methodological option for this region than the standard hydro-meteorological approaches. The latter usually involves greater uncertainty in the evaluation of peak flows, given the peculiarity of storms in this area, with varying intensities, which are heterogeneous in space and very short in time.

In connection with this, the interest of the present study is two-fold: (i) to check the fitness level in these types of methods supported by high resolution DTM and abundant field data as opposed to meteorological methods; and (ii) to show its advantages for the evaluation of historic floods combined with the use of remote sensing techniques. More specifically, the integrated use of remote sensing data, *in situ* data, and digital elevation models, could be particularly useful for obtaining hydraulic geometry data in flooded areas, and, therefore, for estimating discharges, water volumes stored in floodplains and hydraulic regime parameters.

2. Study Area

The present study has been developed in several drainage basins in the Region of Murcia (south-eastern Spain), characterized by a semi-arid climate with heavy rain, the presence of ephemeral channels (*ramblas*) and frequent flooding events. The basins analyzed consisted completely of a group of independent ephemeral drainage areas with a direct outlet to the sea, a predominant dendritic drainage pattern, steep slopes and a torrential regime. This coastal group within the Region of Murcia consists of a total of 53 basins with different sizes, between 0.5 and 522 km^2 (Figure 1). Almost half of them have a very small watershed area of less than 10 km^2, which could be totally covered by just one storm. Another 11 basins are also small areas of less than 30 km^2, which could be completely covered by mesoscale precipitation events, and only six basins are equal to or greater than 70 km^2; those drained by the Albujón, Benipila, Cañarete, Moreras, Pastrana and Ramonete *ramblas*. The most extensive and dangerous, due to their large floods, are the basins of the Albujón (522 km^2), las Moreras (246.5 km^2) and Benipila (147 km^2).

Figure 1. Study area and location of the sectors selected (A to F) for application of hydraulic geometry method (HGM) and remote sensing techniques.

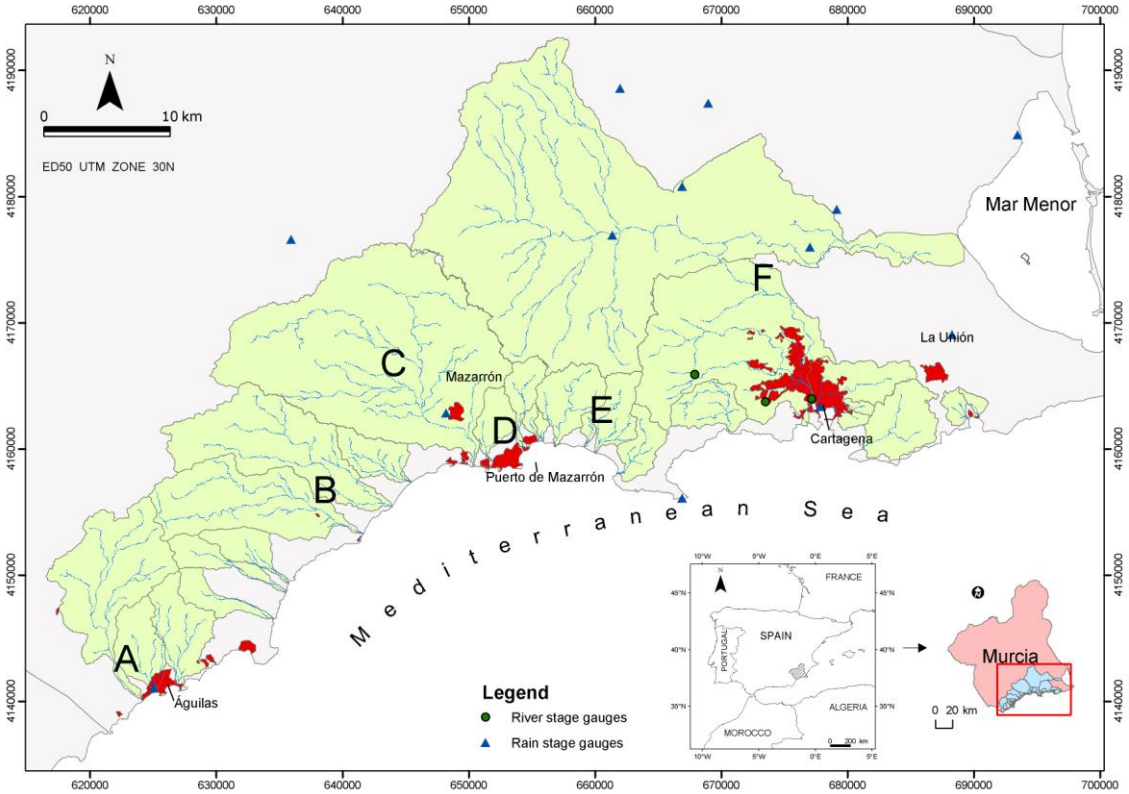

Only a few *ramblas* have discharge data provided by the AHIS. The low reaches of these courses (Benipila Rambla, in Cartagena, and Nogalte Rambla, in Puerto Lumbreras), equipped with AHIS gauging stations, have been used for estimating the flow in recent storms and for checking the accuracy of hydraulic geometry methods (HGM) against hydrometeorological models. However, the methodological proposal to combine HGM with remote sensing techniques has been trialed in coastal areas flooded by the overflowing of torrential watercourses during the intense rains of 23 October

2000. Six *rambla* reaches were studied in this case (letters A to F in Figure 1). These reaches are located in the Cañarete-Charco (A), Ramonete (B), Moreras (C), Lorentes (D), Honda (E) and Benipila-Dolores (F) *ramblas*. All of these have been selected because, in addition to being located in the zones most affected by this hydrological process, enough field data are available to be able to apply the proposed methods. All of these basins are characterized by torrential drainage systems established on steep headwaters of metamorphic materials and low areas with a slight gradient formed by soft sediments (marls, silts and clays).

All of them have been selected because, besides being placed in the sectors most affected by the mentioned hydrological events, they have sufficient field data to apply the proposed methods. All these basins are characterized by ephemeral drainage networks established on steep headwaters of metamorphic terrains and low sectors of scanty slope formed by soft materials (marls, silts and clays). These conditions, together with the existence of a scanty vegetation cover and the action of very irregular and intense rainfall (>50 mm/h), favor the development of large and flash floods.

3. Methodology

Firstly, to determine the validity of the HGM applied to the fluvial systems combined with remote sensing methods, its fitness level has been tested in comparison with the results obtained by hydrometeorological methods (SCS Dimensionless Unit Hydrograph, SCSD, Témez *gamma* Unit Hydrograph Tγ, and the Modified Rational Method, MRM). As comparative data for this validation, discharge values of the AHIS in the gauging stations of Cartagena (Benipila Rambla) and Puerto Lumbreras (Nogalte Rambla) have been used. The confrontation of such methods is carried out using the comparative analysis of 10 important storm events that occurred between 1997 and 2009. Given the best fit of the HGM with real gauging data, this method makes it possible to calculate laminated flows in the flood zones, once water surface is delimited using satellite images according to the methodology described in Bustamante *et al.* [13]. This model is based on obtaining ROIs (Regions of Interest) in areas that show a characteristic water spectral behavior from the differential response between the reflectivities of 4, 5 and 7 channels, and the posterior conversion of these ROIs in vectorial archives. In this study the HGM has been trialed in some of the main areas of flooding observed after the storm on 23 October 2000 (sectors denominated with the letters A to F in Figure 1).

3.1. The Hydraulic Geometry Method (HGM) Compared to Hydrometeorological Methods for Calculating Flood Discharges

3.1.1. Hydrometeorological Models

In order to provide flow information the environment data of each basin were introduced into the hydrometeorological models, especially precipitation values. There are many methods in this respect: pluviometer weights in each subbasin according to Thiessen's method of polygons [14], the rainfall calculation from the distance inverse method, rainfall by cells (meteorological radar), and SCS storms (24 h volume) associated to frequency. In this work daily rainfall data have been used from 16 stations of the National Meteorological Institute (NMI) located at or near to the study area. The types of

hydrograph methods adopted here are: dimensionless Unit Hydrograph (UH) of SCS adjusted to a gamma function [15,16]; Témez's triangular UH; and Témez's modified rational method.

- *SCS Dimensionless Hydrograph Method.* The SCS Dimensionless Unit Hydrograph method has been applied using a rainfall raster map obtained by the spatial interpolation of precipitation data. Using GRASS (*r.statistics command*) the mean precipitation for subbasins has been calculated. A SCS type temporal distribution has been applied to the rainfall quantities in 24 hours, choosing the most adequate temporal interval [17]. The SCS Dimensionless is a synthetic unitary hydrograph in which discharges are expressed in relation to peak flow (q_p), and times in relation to peak time (T_p), once estimated q_p and T_p from the triangular UH of SCS. Studies carried out in the United States in rural basins of various sizes [15], show that the lag time between peak rainfall and peak discharge is about 0.6 times the basin concentration time [18].

- *Témez's Unit Hydrograph Method* (*TUHM*) *and the Modified Rational Method (MRM).* Témez's formulas (*TUHM*) and the Modified Rational Method (*MRM*) use the channel slope to calculate the concentration time which generates values which are lower than those of the SCS, given that the channel slope is always less than the mean of the basin. Témez's triangular UH, in spite of having been used very much in Spain, is usually more appropriate for extreme hydrological events of a large magnitude. What is more, it is a modification of the SCS Triangular UH adapted to local conditions so that the peak discharge, in this case, tends to be bigger and the base time lower [19-21]. In fact, there is a restriction imposed by a unit rainfall time which is less than the fifth part of concentration time, a fact that rules out less torrentiality events. Likewise the rational method applied in this work follows the formula proposed by Témez [19-22] adapted for the climatic conditions in Spain. This method, widely used in Spain, is known as the Modified Rational Method (*MRM*) and is able to estimate in a simple way the peak discharges in small and medium basins with concentration times (*Tc*) between 0.25 and 24 hours [22,23].

$$Q_p = (1/3.6)\, C\, I\, A\, K \tag{1}$$

where Q_p ($m^3\ s^{-1}$) is the peak discharge, I (mm h^{-1}) the maximum mean intensity for a duration interval which is equal to concentration time, C the runoff coefficient for the interval in which I is produced, A the area of the drainage basin (km^2) and K the uniformity coefficient. The precipitation analysis has been carried out using the daily precipitation values of storms analyzed in 12 meteorological stations belonging to or near the basins under study. Due to the lack of precipitation intensity-duration-frequency (IDF) curves in the study area, it has been necessary to apply the Norm 5,1-I.C., MOPU's Road Instruction [23] and Ferrer's work [20], in which it is accepted that the hourly and daily intensity ratio is a value 11 times higher for this semi-arid area. With regard to the time of concentration (Tc), this can relate to hourly rainfall intervals because it was estimated before and is included in Equation 2 to obtain I_t (rainfall intensity in this time interval).

$$I_t = I_d \left(\frac{I_1}{I_d} \right)^{\frac{28^{0,1} - t^{0,1}}{28^{0,1} - 1}} \tag{2}$$

where I_d = Mean daily rainfall intensity (daily P/24 hr); I_1 = Rainfall intensity in the most rainy hour; t = Time interval (h) to evaluate the rainfall intensity.

To correct the fact that the spatial rainfall distribution is not uniform, the area reduction coefficient has been used (ARC) proposed by Témez [22], through the expression *1 − ((log A)/15)*, where A is the area of the basin (km^2). The possible errors generated by the lack of uniformity of net rainfall over time are corrected using a uniformity coefficient that varies according to concentration times. The runoff coefficient is a result of the relationships between daily precipitation and runoff threshold (P_0), the latter obtained from the land uses and soil hydrological characteristics.

3.1.2. Channel Hydraulic Geometry Methods

HGMs have been used frequently in the reconstruction of palaeofloods [24-26]. They are generally based on the identification in the field of indicators of water height during flooding which together with geometric characteristics of the channel section are used in standard hydraulic calculations for estimating peak flows. In this study, two calculation methods have been applied, according to the hydraulic conditions of each reach: (1) The critical depth method in those sections that experienced an abrupt change in the slope and it is assumed therefore that there are critical flow conditions during flooding; and (2) the Manning equation commonly used in well-defined open channels, adopting Jarrett's approach [27-29] for the calculation of the roughness coefficient in reaches with a steep slope. The reaches to which these equations have been applied in the analyzed channels have very varied slope ranges, between 0.007 and 0.039 ($m\ m^{-1}$). The critical depth used here for channels with steep slopes (>0.02 m m-1) is the one proposed by Jarrett [29] according to the expression:

$$Q\ (m^3\ s^{-1}) = Ac\ Vc \quad (3)$$

where *Ac* is the area of the section and *Vc* the critical velocity. Using Jarrett's formula [28,29] proposed for the calculation of the bed roughness in steep reaches ($n = 0{,}32R^{0{,}38}\ S^{-0{,}16}$), in such cases Manning's equation has been reformulated estimating the flow velocity and the flood discharge from the expressions:

$$V = 3.17\ R^{0.83}\ S^{0.12} \quad (4)$$

$$Q = 3.17\ AR^{0.83}\ S^{0.12} \quad (5)$$

where *V* is the mean flow velocity ($m\ s^{-1}$), *Q* the peak discharge ($m^3\ s^{-1}$), *A* the area of the wet cross-section (m^2), R the hydraulic radius (m) and S the slope of the water surface (or the bed slope in relatively uniform channels) [30]. In the validation of HGM several cross-sections have been used which are located upstream from the AHIS control stations (lower reaches of the Benipila and Nogalte *ramblas*). However, for the estimation of laminated discharges through the studied flood (23 October 2000) a total of 63 topographic profiles have been extracted and grouped by series within the six flooding sectors defined using Landsat images. The first two series of cross-sections correspond to flooded sectors in the lower reaches of the Cañarete and Charco *ramblas* (Águilas) (sector A), the third series was located in the mid-low reach of the Ramonete rambla (sector B), the fourth and fifth are extracted from sectors C and D flooded by the Moreras and Lorentes *ramblas* respectively.

The E sector is made up of two series of profiles, located to the right and left of the final reach of the Valdelentisco Rambla, while sector F is made up of another two series running along both sides of the Dolores-Benipila Rambla.

3.2. Combination of Hydraulic Geometry Methods (HGM) with Remote Sensing Methods for Recent Floods

The measurement of the direct discharge is difficult and very costly, which is why indirect procedures are often used based on measuring the water level and hydraulic geometry data with cost curves known *a priori*. This is the case of the AHIS, which through various sensors and devices (float and counterweight, piezoresistives, compact tire, ultrasound and radar) makes it possible to measure the height of water and to obtain relatively precise hydraulic data from periodic record campaigns. In ephemeral channels, it is quite common to calculate peak flood discharges by applying hydraulic models based on channel geometry data, area of the wet cross-section, longitudinal slope and bed roughness (methods based on hydraulic geometry), but the level of precision is not so high. Even so, they could generate good results if the used topographic and roughness data have high quality. The limits of the flooded areas in the flood in October 2000 have been established using the analysis of Landsat images. These areas are defined by polygons from a planimetric information layer without heights, through vectorial files (.shp and .evf formats). To obtain the water heights in these sectors, the masks extracted through remote sensing techniques have been superimposed on a digital terrain model. The DTM used is one of the products of a digital photogrammetric flight financed in 2008 by the Agriculture and Water Ministry of the Region of Murcia. The basic reference system of the whole project is ETRS89, supported by the REGENTE network through the permanent Meristemum GNSS stations. In this flight a LIDAR rising was carried out (Figure 2), of which DTM is derived (4 × 4 m) and used here, with more precision than the traditional automatic correlation photograms. For the specific case of flat zones that have been flooded, it is very useful to have LIDAR pulses available to complete the information provided by the DTM, given that precision is greater in a small space.

The Hec-RAS program and its Hec-GeoRAS extension for ArcView3.x have been used for the hydraulic modeling. Specifically from this extension, a total of 63 cross-section profiles have been extracted which have served to determine the geometric features of the analyzed flood areas. On the DTM (transformed into a model of elevations obtained by Triangular Irregular Network—TIN) the channel and the cross-sections are drawn up, generating a 3D file containing elevations and distances with regard to the adjacent profiles. By superimposing the flooded areas defined using remote sensing onto the model of elevations (TIN) a raster map was obtained, with the same cell size as the one chosen in the file exportation which provides data about the flow width and depth. The roughness data have also been included in this file, with the addition of a polygon layer on land uses that represent different Manning "n" roughness values (Table 1). Already in Hec-RAS, discharges—which cover the wet perimeter sections—are simulated through steady flow analysis, considering that being floodplains, the flow regime tends to be subcritical and the roughness somewhat higher than in the channel, as reflected in its predominant uses (scrubs, crops under plastic, and trees). The use of multiple profiles in the flow analysis allows to select the best profiles that adjust at the flooded area.

Figure 2. LIDAR rising. Flight financed in 2008 by the Agriculture and Water Ministry of the Region of Murcia.

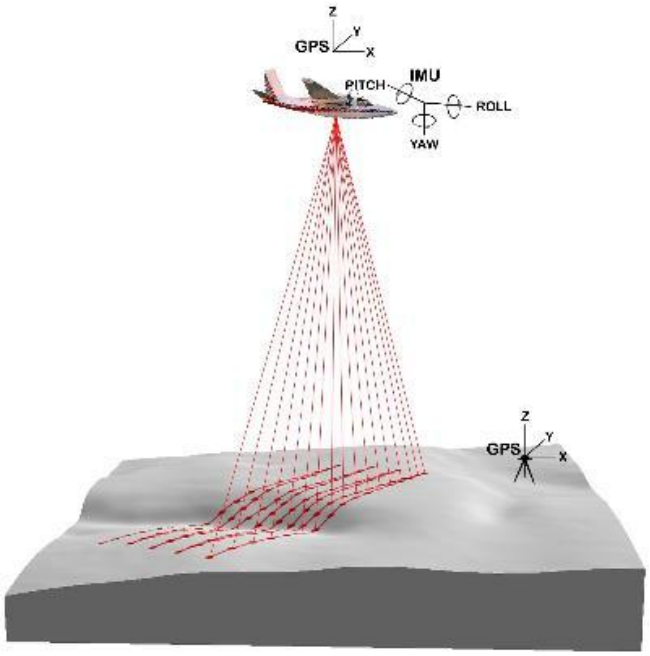

Table 1. Manning roughness values used in the analysis. U. S. Army Corps of Engineers, Hydrologic Engineering Center [32].

Type of Channel and Description	Minimum	Normal	Maximum
A. Natural Streams			
1. Main Channels			
a. Clean, straight, full, no rifts or deep pools	0.025	0.030	0.033
b. Same as above, but more stones and weeds	0.030	0.035	0.040
c. Clean, winding, some pools and shoals	0.033	0.040	0.045
d. Same as above, but some weeds and stones	0.035	0.045	0.050
e. Same as above, lower stages, more ineffective slopes and sections	0.040	0.048	0.055
f. Same as "d" but more stones	0.045	0.050	0.060
g. Sluggish reaches, weedy, deep pools	0.050	0.070	0.080
h. Very weedy reaches, deep pools, or floodways with heavy stands of timber and brush	0.070	0.100	0.150
2. Flood Plains			
a. Pasture no brush			
1. Short grass	0.025	0.030	0.025
2. High grass	0.030	0.035	0.050
b. Cultivated areas			
1.No crop	0.020	0.030	0.040
2. Mature row crops	0.025	0.035	0.045
3. Mature field crops	0.030	0.040	0.050
c. Brush			
1. Scattered brush, heavy weeds	0.035	0.050	0.070
2. Light brush and trees, in winter	0.035	0.050	0.060

Table 1. *Cont.*

Type of Channel and Description	Minimum	Normal	Maximum
3. Light brush and trees, in summer	0.040	0.060	0.080
4. Medium brush and trees, in winter	0.045	0.070	0.110
5. Medium brush and trees, in summer	0.070	0.100	0.160
d. Trees			
1. Cleared land with tree stumps, no sprouts	0.030	0.040	0.050
2. Same as above, but heavy sprouts	0.050	0.060	0.080
3. Heavy stand of timber, few down trees, little undergrowth, flow below branches	0.080	0.100	0.120
4. Same as above, but with flow into branches	0.100	0.120	0.160
5. Dense willows, summer, straight	0.110	0.150	0.200
3. Mountain Streams, no vegetation in channel, banks steep, with trees and brush on banks submerged			
a. Bottom: gravels, cobbles and few boulders			
b. Bottom: cobbles with large boulders			
B. Lined or Built-Up Channels			
1. Concrete			
a. Trowel finish	0.011	0.013	0.015
b. Float Finish	0.013	0.015	0.016
c. Finished, with gravel bottom	0.015	0.017	0.020
d. Unfinished	0.014	0.017	0.020
e. Gunite, good section	0.016	0.019	0.023
f. Gunite, wavy section	0.018	0.022	0.025
g. On good excavated rock	0.017	0.020	
h. On irregular excavated rock	0.022	0.027	
2. Concrete bottom float finished with sides of:			
a. Dressed stone in mortar	0.015	0.017	0.020
b. Random stone in mortar	0.017	0.020	0.024
c. Cement rubble masonry, plastered	0.016	0.020	0.024
d. Cement rubble masonry	0.020	0.025	0.030
e. Dry rubble on riprap	0.020	0.030	0.035
3. Gravel bottom with sides of:			
a. Formed concrete	0.017	0.020	0.025
b. Random stone in mortar	0.020	0.023	0.026
c. Dry rubble or riprap	0.023	0.033	0.036
4. Brick			
a. Glazed	0.011	0.013	0.015
b. Incement mortar	0.012	0.015	0.018
5. Vegetal lining	0.030		0.050
C. *Excavated or Dredged Channels*			
1. Earth, straight and uniform			
a. Clean, recently completed	0.016	0.018	0.020

Table 1. *Cont.*

Type of Channel and Description	Minimum	Normal	Maximum
b. Clean, after weathering	0.018	0.022	0.025
c. Gravel, uniform section, clean	0.022	0.025	0.030
d. With short grass, few weeds	0.022	0.027	0.033
2. Earth, winding and sluggish			
a. No vegetation	0.023	0.025	0.030
b. Grass, some weeds	0.025	0.030	0.033
c. Dense weeds or aquatic plants	0.030	0.035	0.040
d. Earth bottom and rubble side	0.028	0.030	0.035
e. Stony bottom and weedy banks	0.025	0.035	0.040
f. Cobble bottom and clean sides	0.030	0.040	0.050
3. Dragline-excavated or dredged			
a. No vegetation	0.025	0.028	0.033
b. Light brush on banks	0.035	0.050	0.060
4. Rock cuts			
a. Smooth and uniform	0.025	0.035	0.040
b. Jagged and irregular	0.035	0.040	0.050
5. Channels not maintained, weeds and brush			
a. Clean bottom, brush on sides	0.040	0.050	0.080
b. Same as above, highest flow stage	0.045	0.070	0.110
c. Dense weeds, high as flow depth	0.050	0.080	0.120
d. Dense brush, high stage	0.080	0.100	0.140

The delimitation of flooded areas defined from Landsat images immediately after the flood of 23 October, 2000 have been contrasted with the marked limits, according to hydromorphological criteria, through the bankfull discharges and flood prone areas. This has made it possible to catalogue these extreme hydrological events depending on the reached morphological thresholds (main channel associated with dominant discharges and active floodplains) and therefore to determine the hazard levels.

3.3. Using Bankfull Stage and Flood-Prone Area as Thresholds of Flood Hazard

For the analysis of bankfull and flood prone areas, 150 cross-sections along the middle and lower reaches in the studied coastal *ramblas* have been obtained, between Águilas and Cartagena. The measurement of these cross-sections was carried out using TOPCON Hiper+ GPS, the TOPCON FC100 notebook and the INLAND group Triton program. Cross-sections were located in straight or non-sinuous reaches with uniform depth, avoiding proximity of gully junctions and turbulent sectors. Channel width, maximum and mean depth, wetted perimeter, entrenchment ratio, and bankfull and

flood-prone areas were measured in three to four locations within the survey reach and averaged to produce representative reach values.

4. Results and Discussion

4.1. Validation of the Hydraulic Geometry Method compared to the Rainfall-Runoff Models

Table 2 shows the main morphometric data of the basins and channels used in the validation of described methods, in addition to its respective runoff thresholds (P_0) and curve numbers (CN). The influence of the lithological control in runoff indexes is notable because the metamorphic basin of Nogalte has a greater curve number and a lower P_0 than the limy basin of Benipila, in spite of it having a higher mean slope. However, the characteristic times of the unit hydrograph vary according to the method applied. Témez's UH methods and MRM offer very similar values, which are always greater in the Nogalte Rambla (Table 3). On the other hand, the time of concentration, lag time and time to peak estimated for the SCS UH method are shorter in this rambla and slightly longer in the Benipila Rambla, which denotes a greater influence of the soil infiltration capacity compared to the other hydrological abstractions.

Table 2. Morphometric parameters of basins and channels and curve numbers (CN) used for elaborating unit hydrographs. Watercourses included in the study area.

Basin	Watershed area (km^2)	Basin slope (m/m)	Channel length (km)	Channel slope (m/m)	P_0 (mm)	CN
Benipila	97.10	0.1370	22.84	0.016	34.3	81.4
Benipila+Dolores	144.64	0.1145	24.35	0.013	26.9	84.8
Nogalte	128.65	0.1943	32.40	0.022	23.2	86.6

P_0 = runoff threshold; CN = curve number.

Table 3. Characteristic times of the unit hydrograph obtained for each watershed area from the SCS Dimensionless UH method (SCSD), Témez's *Gamma* HU (T_γ) and the Modified Rational Method (MRM).

Rambla	Tc (h)			Lt (h)			Bt (h)			Tp (h)		
	A_{SCS}	T_γ	MRM	A_{SCS}	T_γ	MRM	A_{SCS}	T_γ	MRac	A_{SCS}	T_γ	MRM
Benipila	4.33	7.09	7.09	2.60	2.48	2.60	13.19	15.15	7.57	2.68	2.57	2.68
Benipila + Dolores	4.45	7.75	7.75	2.67	2.71	2.67	13.54	16.52	8.23	2.71	2.75	2.71
Nogalte	4.02	8.71	8.71	2.41	3.05	2.83	12.27	18.54	9.15	2.45	3.09	2.45

tc = time of concentration; lt = lag time; bt = base time; tp = time to peak.

The flood peak discharges obtained using hydrometeorological methods are in many cases different from those facilitated by the AHIS (Table 4). The main cause is supported by the condition of homogenous rainfall on which rainfall-runoff models are based, especially the unit hydrograph method (UHM). The locally strong storms on the middle-lower reach, where the observatories with

pluviographs are located, lead to high values which could generate small flows because they are not representative episodes of the basin.

Table 4. Flood peak discharges estimated using the SCS Dimensionless UH method (SCSD); Témez's *Gamma* HU (T_γ); Modified Rational Method (MRM); and the Hydraulic Geometry Method (HGM); compared with the peak flows measured by AHIS.

Rambla	Date	Peak discharge (m^3/s)				basin P (mm)	Q AHIS (m^3/s)
		SCSD	Tγ	MRM	HGM		
Benipila	30/09/1997	9.5	9.3	16.8	2.3	54.7	2.9
	23/10/2000	477.0	468.1	272.7	405.9	162.8	430.7
	18/11/2003	282.8	277.6	208.4	57.5	141.1	1.2
	16/04/2004	68.8	67.7	99.5	3.1	98.7	5.5
	09/10/2008	184.9	183.1	88.7	9.6	93.8	0.9
Benipila+Dolores	09/10/2008	294.1	282.5	164.1	9.6	93.8	0.9
	28/09/2009	288.5	275.7	525.9	258.2	176.8	271.6
Nogalte	29/09/1997	50.7	40.3	77.3	45.7	67.1	53.9
	09/10/2008	--	--	18.8	24.1	39.2	28.3
	13/09/2009	1.4	1.0	15.0	29.9	36.7	37.6

P = Precipitation; Q = Discharge.

$$Q_{AHIS} = 1.0706\ Q_{HGM} - 7.243 \qquad (R^2 = 0.98) \tag{6}$$

$$Q_{AHIS} = 0.6348\ Q_{MRM} - 11.064 \qquad (R^2 = 0.46) \tag{7}$$

$$Q_{AHIS} = 0.7401\ Q_{T\gamma} - 52.463 \qquad (R^2 = 0.49) \tag{8}$$

$$Q_{AHIS} = 0.7322\ Q_{ASCS} - 55.637 \qquad (R^2 = 0.50) \tag{9}$$

The interpolation of the rainfall intensity data of this reach with others with less detail in the rest of the basin, introduces an error factor that is often appreciable. In fact, the location of the meteorological stations in the Benipila basin, in an area of less than 10 km^2 near the city of Cartagena (lower reach) which hardly accounts for 10% of the whole watershed area, together with the lack of pluviometric information in the headwater area, means that the unit hydrograph method (UHM) is scantily satisfactory when storms are slightly extended. In these cases, the basin surface of the study is too wide to be completely affected by isolated storms which are mainly of a convective origin.

Only when the storms are sufficiently generalized, affecting most of the basin with low intensities, do these methods provide acceptable approximations. The following are examples of this: the storms of 30 September, 1997, 23 October, 2000 and 28 September, 2009 for the Benipila Rambla basin and 29 September, 1997 for the Nogalte Rambla basin (Table 4). However, these methods overestimate peak flow even more when the measured value is higher. The Dimensionless UH with SCS *gamma* function (SCSD) usually provides values between 6 and 11% higher than those registered by the AHIS, while Témez's *Gamma* HU (T_γ) gives values which are between 2 and 9% higher. The MRM shows values that are less fitted despite correction factors applied.

The best-fit with the AHIS data is provided by the HGM, with a determination coefficient $R^2 = 0.98$. This explains why the AHIS determines the discharges using cost curves associated to water levels, having a close correlation with geometric parameters of the channel cross-sections in which height sensors are installed. There is a linear relationship between both types of values (Equation 6). In most cases the flood peak discharges estimated using the HGM are lower than those measured using AHIS, which is due to the reduced influence of the bed roughness in the AHIS control sections, which are normally channeled and have a flat bottom. The cross-sections used in the calculation of the peak flows with HGM belong to naturally open channels, located immediately upstream from the reaches channeled with AHIS gauging stations.

These natural sections generally have more irregular beds, provided with vegetation and alluvial forms which give it a greater degree of roughness.

In Figure 3 a comparison has been made of the hydrograph calculated using UH methods, the hydrograph construct from AHIS data and the peak discharge estimated by HGM, corresponding to the flood of 23 October, 2000.

Figure 3. Hydrographs obtained using the UH methods and AHIS measurements in comparison to the peak flow estimated by HGM. Flood of the 23 October, 2000.

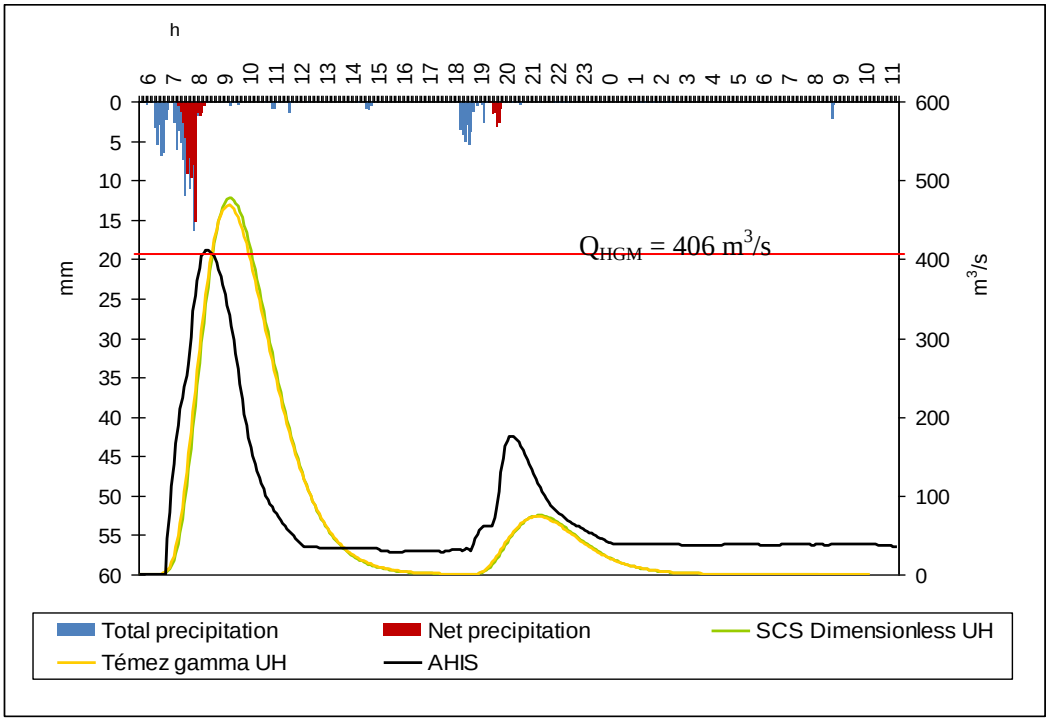

By overestimating the real flood discharges, SCSD and T_γ UH could be used to establish greater safety levels when there are extreme hydrological events. Table 5 shows the hydraulic geometric values extracted using Hec-RAS from the maximum flows estimated using these methods in the three floods of the Benipila Rambla with the best theoretical fits. In these cases, the following hydraulic geometry variables have been obtained: the water sheet width, the mean flow depth, the area of the flow section and the wetted perimeter. The bed slope is determined using the DEM and the cross-section elevations measured by GPS, while the channel roughness (n) is a field data.

Given that we are dealing with the same reach, the slope and the bed roughness are kept constant. The remaining values closely reflect flow variations and are somewhat higher when the flood simulation is run with SCSD UH. However, the difference between the hydraulic geometry values obtained using SCSD UH and T_γ UH discharges is minimal in large floods and practically inexistent in small floods.

Table 5. Hydraulic geometry data of the peak flow on 23 October, 2000 estimated using the SCS Dimensionless UH method (SCSD) and Témez's *Gamma* HU (T_γ). AHIS station of the Benipila Rambla through Cartagena.

Rambla	Date	Q	h (m)	W (m)	A (m^2)	wP (m)	V (m/s)	S (m/m)	n
Benipila	30/09/1997	SCSD	0.28	20.5	5.71	20.6	1.66	0.0025	0.04
		Tγ	0.28	20.4	5.64	20.5	1.65	0.0025	0.04
Benipila	23/10/2000	SCSD	2.18	47.8	103.24	48.0	4.61	0.0025	0.04
		Tγ	2.16	47.2	101.97	47.9	4.58	0.0025	0.04
Benipila - Dolores	28/09/2009	SCSD	1.59	46.0	73.10	46.5	3.93	0.0025	0.04
		Tγ	1.55	45.8	70.90	46.3	3.88	0.0025	0.04

Q = discharge; h = flow depth; W = flow width; A = wet cross-section area; wP = wet channel perimeter; V = flow velocity; S = channel slope; n = bed roughness.

4.2. Application of the Proposed Methodology

With the help of satellite images, it has been possible to reconstruct flooded areas in the study *ramblas*. Comparison of the bankfull limits and flood-prone area established using field work and DEM could prove whether the magnitude of a given flood is greater than the hazard thresholds defined according to hydromorphological criteria.

In the flood used as an example for the application of the proposed methodology, of 23 October 2000, the extension of the water sheet and the energy developed by this flood exceed the flood-prone area thresholds at several points. In the case of Lorentes Rambla (Figure 4), it is clear that there is a greater surface covered by this flood compared to the limits marked by the flood-prone area, especially in the final reach. Even the discharge calculated for the same event and reach using HGM, applied to the delimitation of the flooded area from Landsat images, it is twice larger than the discharge in the flood-prone area (Table 6).

As Table 6 shows, the Q_{HGM}*/Q(fp) ratio of all the analyzed cases is between 1.6 and 2, which clearly shows the high rate of hydrological and morphological hazard of the studied flood, especially due to the great width and depth reached by its waters. The width and depth of the channel in the bankfull and flood-prone area stages vary longitudinally according to the hydraulic regime variations, the geological constrictions and the grain-size distribution. This could explain why the area affected by the flood on 23 October, 2000 is downstream considerably different to the flood-prone area. In the end reach, the Lorentes Rambla has a channel that is constrained by protective walls and buildings which invade the floodplain, in such a way that the width of the flood-prone area is only slightly different from the bankfull width and is widely exceeded by the width of the flooded area in this event.

Figure 4. Delimitation of the flood area on 23 October, 2000 compared to the flood prone area. Lower reach of the Lorentes Rambla.

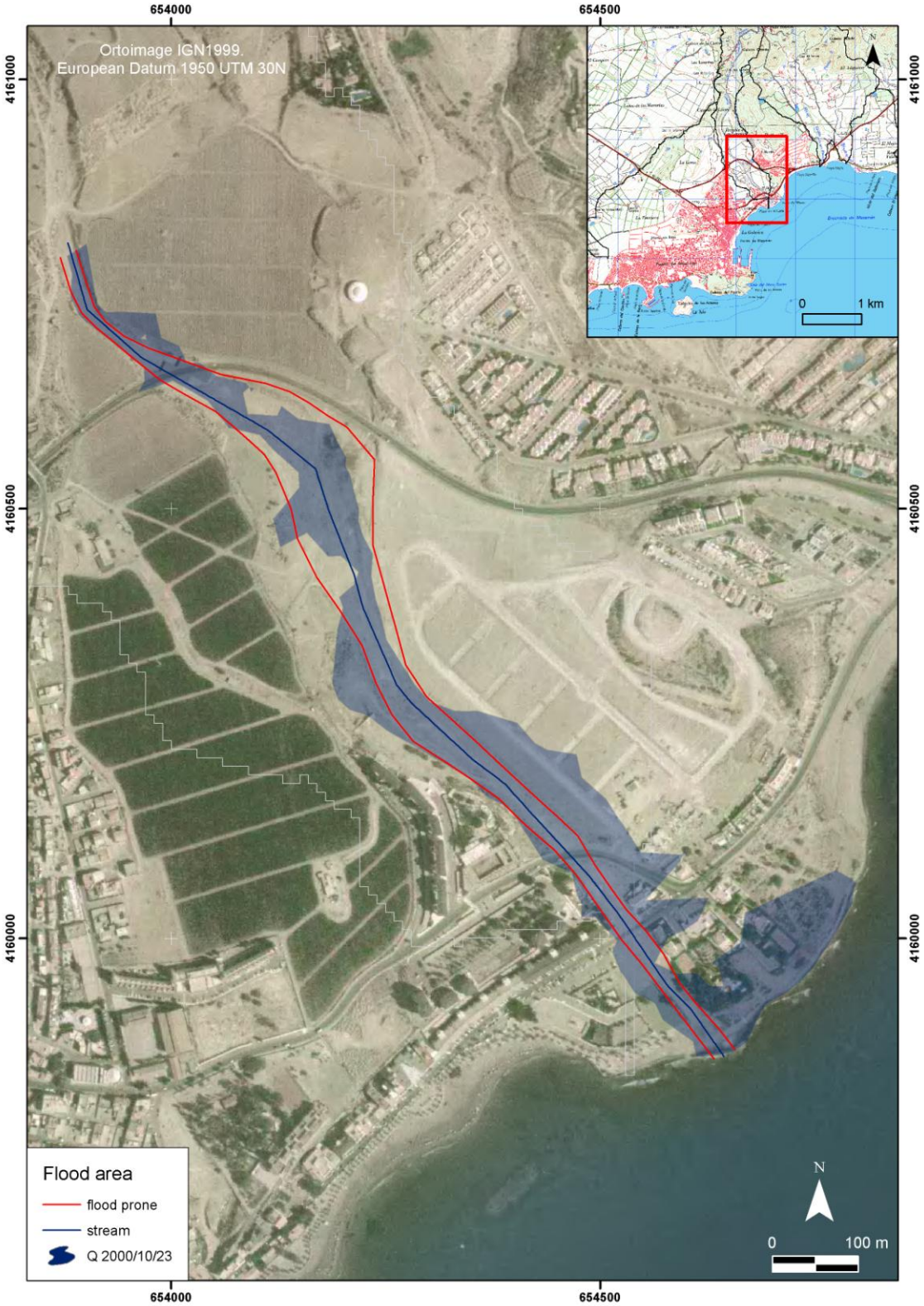

Table 6. Comparison of HGM flow estimated for the flood of October 2000 with predicted flood-prone area discharge in the study cross-sections.

ID	W (fp)	h_m (m)	A (m^2)	h_{max} (m)	S	n	Vm (m/s)	Q(fp) (m^3/s)	Q_{HGM}* (m^3/s)	Q_{HGM}*/Q (fp)
R4	138	0.77	106.3	1.78	0.0100	0.053	1.59	168.4	277.0	1.64
Vi3	38	0.45	17.1	1.66	0.0191	0.052	1.56	26.6	42.4	1.59
L3	59	0.49	28.9	0.62	0.0069	0.029	1.79	51.8	104.6	2.02
B19	178	0.95	169.1	2.13	0.0025	0.040	1.21	204.3	405.9	1.99

W(fp) = flood prone width; h_m = flow mean depth; A = wet cross-section area; h_{max} = flow maximum depth; S = channel slope; n = bed roughness; Vm = flow mean velocity; Q(fp) = discharge in flood prone area; Q_{HGM}* = discharge estimated from HGM.

In bankfull conditions more than 58% of the culvert systems located on the road-stream crossings is incapable of evacuating flood waters, a percentage which increases to 88.2% when the flow reaches the flood-prone stage. However, the drainage capacity of these works is often greatly reduced due to the obstruction caused by the bedload transport, especially in *ramblas* with strong slopes close to sediment sources (e.g., the Ramonete and Pastrana *ramblas*). The greatest hazard is found in the stream ford reaches crossed by roads, where the hydraulic and morphological processes of the flood maintain their continuity.

In extreme floods, where the flood-prone area is completely covered, the bed of these reaches is very unstable, registering Relative Bed Stability (RBS) values and Log Relative Bed Stability (LRBS) values which are often below 0.25 and −0.60 respectively [32]. This bed instability means that these reaches also have greater potential bed transport ($6.5 \cdot 10^{-3}$–0.013 m^2/s) [34].

The morphological adjustments produced by the flood on 23 October, 2000 (scour holes, bank erosion, spill-over lobes and lateral accretion deposits in the floodplain) overpass the flood-prone area limits and affect the overall fluvial system. In the main channel the flow caused minor changes, from undercutting of bank base and toppling to morphological bed variations associated with the mobility of alluvial bars and other bedforms. Most of these morphological adjustments are superficial changes which are easily observed *in situ*. What is more difficult to detect is channel bottom erosion (transitory bed erosion), the cause of direct and indirect effects which could damage or endanger the stability of exposed hydraulic structures. The highest transitory erosion values were registered in the lower reach of the Moreras Rambla near Mazarrón, where it was above 1 m. Under the hydraulic conditions that characterized this flood, in nearly 47% of the analyzed reaches, transitory erosion values were above 0.6 m, making this the minimum critical threshold for the design of existing drainage works and those planned in these cases.

The comparison of the anterior and posterior Landsat images in flood events has made it possible to define their spread. Landsat 7-ETM+ false color images showing the meridional coastal *ramblas* of the Murcia Region on 8 August and 27 October, 2000, that is to say 75 days before and four days after the October flood, have been compared. Figures 5 and 6 are an example of this comparison of images before and after the flood on October 2000 in the Cañarete and Charco rambla systems.

Figure 5. False color composition (4, 5, 7) of a Landat 7-ETM+ image on 8 August, 2000 (left) and on 27 October, 2000, 4 days after the flood (right). Lower reach of the Cañarete Rambla (Águilas area).

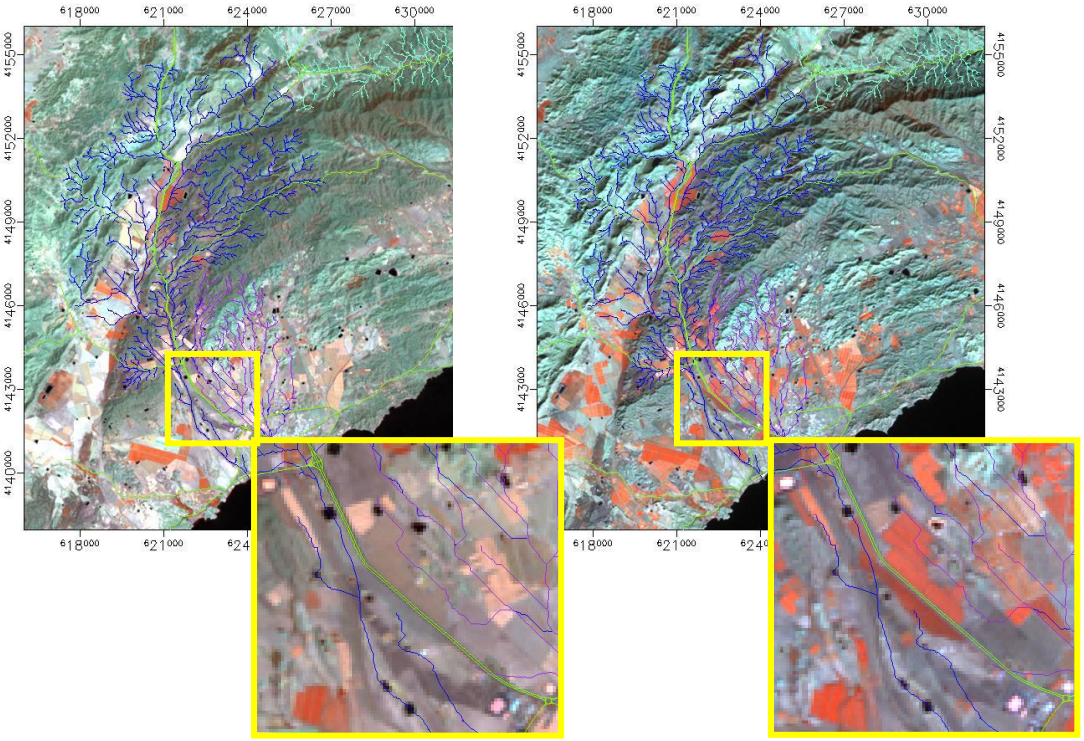

Figure 6. False color composition (4, 5, 7) of a Landat 7-ETM+ image on 8 August, 2000 (left) and on 27 October, 2000, 4 days after the flood (right). Middle-lower reach of the Charco Rambla (Águilas area).

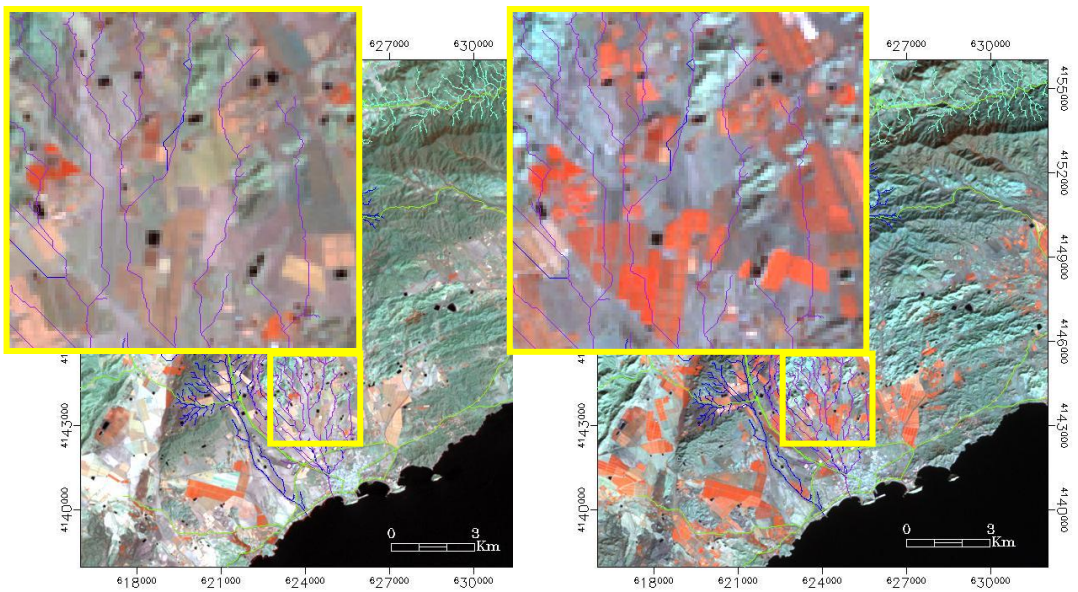

Figure 7. Delimiting of flooded areas after the event on 23 October, 2000 from Landat 7-ETM+ images and location of cross-sections. South coastal zone of the Murcia Region.

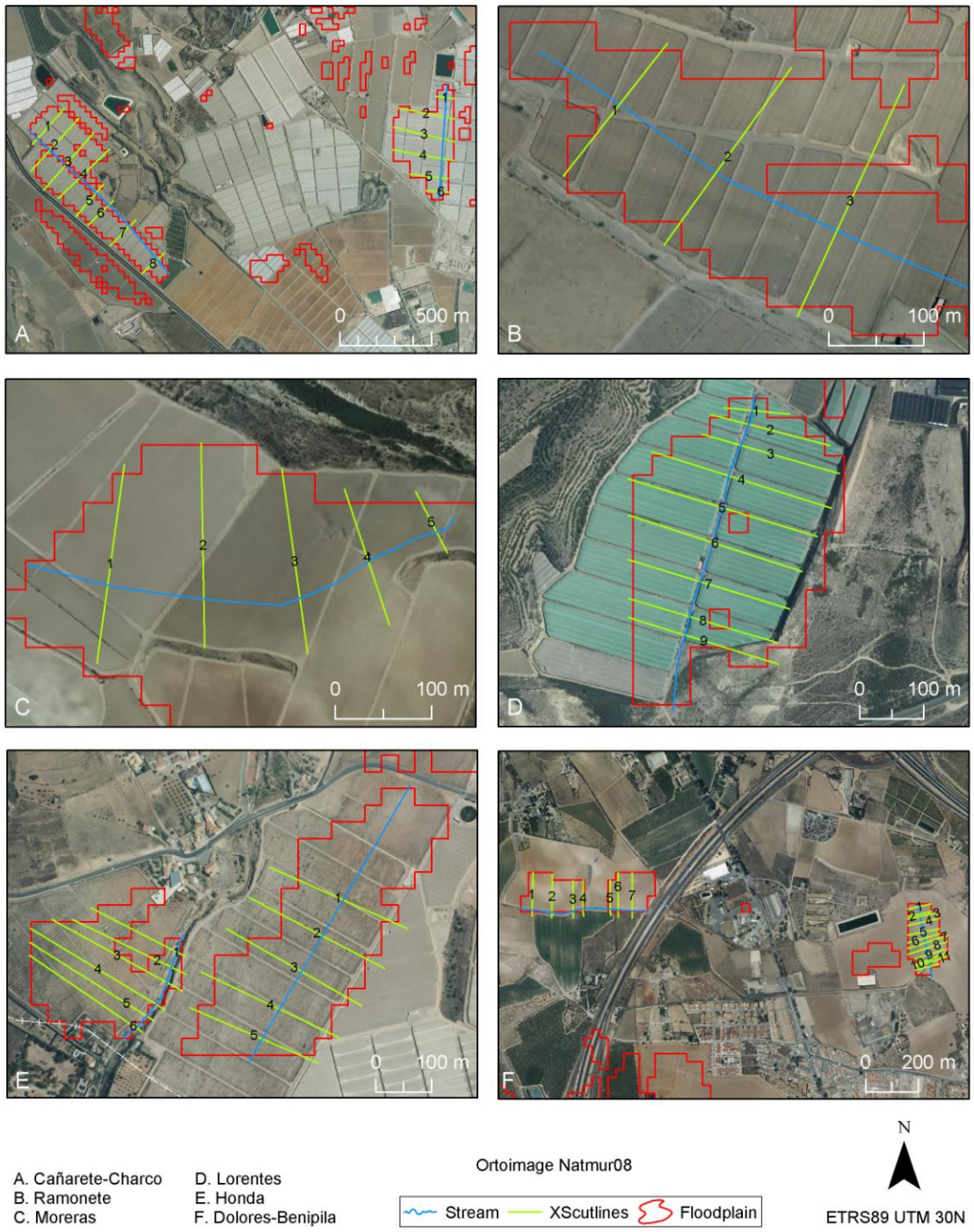

Using these images it has been possible to obtain vector files with information about the limits of the flooded sectors. Figure 7 shows the flooded areas to which the described methodology has been applied and Table 7 has geometric data of different cross-sections representing the water layer in these areas.

The sectors analyzed are residually flooded areas included within the area reached by the flood waters on 23 October, 2000. The residual water sectors delimited using the false color

Landsat 7-ETM+ images on 27 October, 2000, four days after the flood, corresponded to the most depressed topographic areas and most impermeable terrains. The water remains a long time in these areas, increasing the danger for activities and land uses developed there. Water therefore remains on the floodplain adjacent to the study *ramblas*.

Table 7. Geometric and hydraulic parameters of several flooded sectors after the event of 23 October, 2000. South coastal *ramblas* in the Murcia Region.

Flooded sector	h (m)	W (m)	W/h	Rh (m)	V_i (m/s)	Re ($1 \cdot 10^4$)	Fr	A (Ha)	Volume (m^3)
A.1Cañarete	0.30	133.1	447	0.30	1.5	33,51	0.86	21.96	65331
A.2 Charco	0.27	138.1	512	0.27	0.6	13,43	0.39	13.32	35964
B. Moreras	0.37	97.1	260	0.37	1.7	51,75	0.90	8.17	30556
C. Ramonete	0.74	162.3	220	0.74	1.2	69,12	0.45	7.36	54219
D. Lorentes	1.09	75.7	70	0.96	0.9	66,81	0.28	10.26	111720
E.1. Honda (iz)	0.95	192.5	203	0.81	1.9	118,29	0.68	11.16	105797
E.2. Honda (der)	1.34	246.5	183	1.20	0.9	159,48	0.18	4.5	60450
F.1. Dolores (iz)	0.06	98.4	1575	0.06	0.6	2,81	0.73	3.15	1969
F.2. Dolores (der)	0.54	80.1	147	0.54	2.6	104,86	1.12	5.4	29391

Rh = hydraulic radius; V_i = flow initial velocity; Re = Reynolds number; Fr = Froude number.

By applying HGM to these flooded sectors it was possible to reconstruct not only the geometric features of the stored water mass but also the initial conditions of its hydraulic regime. The hydraulic geometry in these residual water bodies varies from case to case. In some areas, water accumulation reaches a mean depth of 1 m and a width greater than 240 m (e.g., right floodplain of the Honda Rambla, sector E2), and in others, such as sectors C and E1, the water ponds have between 0.75 and 1 m depth and between 150 and 200 m mean width. Sector D, located around the Lorentes Rambla, adopts the shape and surface of a group of greenhouses installed on the same floodplain and the same occurs, although at a lower water height (around 0.3 m), in sectors A1 and A2, affected by the overflow of the Cañarete and Charco *ramblas* respectively. Finally, there are areas where the flow lamination diffuses to a wide area of very shallow waters. This is the case for sector E1 located on the left of the Dolores Rambla, to the north of the city of Cartagena. In spite of it being a floodplain depression with a high slope (S = 0.02), the flood did not have the same magnitude here as in the south west of the Region.

It is not surprising that some of these sectors (B and F1), which are sloping, register geomorphic processes that are especially active during the rising flood stage. Very high W/h ratios ($250 < W/h < 1{,}600$) are added to mean significant slope values ($0.02 < S < 0.027$) in these cases, which suggests there is a progressive widening of the erosion grooves generated in the lateral floodplains. These grooves tend to become wider due to the instability of their banks and the crossover of many of these in extraordinarily high waters which leads to higher W/h ratios. This relationship between flow width and depth is greater, although slows as the discharge increases, and it is clearly affected by the lateral erosion of grooves and other active channels within the floodplain. This

widening involves a reduction in the unit flow in the initial sheeting stage, at the same time as more solid material comes into play, causing sedimentary accretion and, therefore, an even greater W/h ratio.

The hydraulic regime that dominated the water entry in the floodplains was subcritically turbulent in nearly all cases as shown by Reynolds' ($Re > 30 \cdot 10^4$) and Froude's numbers ($Fr < 0.9$) (Table 7). The celerity of the surface water waves did not exceed, except in sector F2 (right plain of the Dolores Rambla), the flow velocity during the overflow stage and the high waters were quite calm on these plains.

5. Conclusions

Based on high quality topographic and bed roughness data, the integrated use of hydraulic geometry methods and remote sensing has proven to be a good option for finding out about the characteristics of the water masses in flooded areas close to ephemeral fluvial systems. Its main advantage compared to hydrometeorological ones, for the calculation of flood discharges, is the absence of uncertainties inherent in irregular temporal and spatial distribution of precipitation in the basins that drain these systems. However, the HGM described is only applicable for recent extreme hydrological events, as it requires timely field work to obtain more reliable entry data related to the height of the water observed on the markings in the channels, the bed roughness, and the geometry of cross-sections reconstructed using topographic data which improves the detail of the DTM. The delimitation of the residual flood zones by obtaining the ROIs from the differential reflectivity response between channels 4, 5 and 7, with the help of DTM and the transversal profiles, has served to establish the hydraulic geometry of these areas. The HGM-remote sensing data integration model (Landsat-TM5 and Landsat-ETM+7) also makes it possible to estimate: (a) the hydraulic regime of the flow once it overflows and (b) the volumes of water stored in the floodplains.

Acknowledgments

This paper was carried out within the research project PROMETEO/2009/086, funded by Generalitat Valenciana, and the project RIFLUTME (Natural hazard processes associated with torrential fluvial systems in Mediterranean Environment, application to South Coastal Streams in the Murcia Region), financed by *Fundación SENECA*, Agencia de Ciencia y Tecnología de la Región de Murcia, Reference 02955/PI/05.

References and Notes

1. Lacey, G. Stable channels in alluvium. *ICE Minutes Proc.* **1930**, *229*, 259-284.
2. Lacey, G. Uniform flow in alluvial rivers and canals. *ICE Minutes Proc.* **1934**, *237*, 421-453.
3. Tinkler, K.J. A hydraulic geometry of rockbed channels based on critical flow. In *Proceedings of Geological Society of America Annual Meeitng*, Toronto, ON, Canada, October 25–29, 1998.
4. Dingman, S.L.; Sharma, K.P. Statistical development and validation of discharge equations for natural channels. *J. Hydrol.* **1997**, *199*, 13-35.

5. Leopold, L.B.; Wolman, M.G.; Miller, J.P. *Fluvial Processes in Geomorphology*; W.H. Freeman: New York, NY, USA, 1964.
6. Koblinsky, C.J.; Clarke, R.T.; Brenner, A.C.; Frey, H. Measurement of river level with satellite altimetry. *Water Resour. Res.* **1993**, *29*, 1839-1848.
7. Smith, L.C.; Isacks, B.L.; Bloom, A.L.; Murray, A.B. Estimation of discharge from three braided rivers using synthetic aperture radar satellite imagery. *Water Resour. Res.* **1996**, *32*, 2021-2034.
8. Massonet, D. Satellite radar interferometry. *Sci. Amer. Mag.* **1997**, *February*, 46-53.
9. Riggs, H.C. Flash flood potential from channel measurements. In *Proceedings of Flash Floods Symposium*, Paris, France, September 1974; International Association of Hydrological Sciences Publication No. 112, 1974; pp. 52-56.
10 Osterkamp, W.R.; Hedman, E.R. *Perennial-Streamflow Characteristics Related to Channel Geometry in Missouri River Basin*; Professional Paper 1242; United States Geological Survey: Washington, DC, USA, 1982.
11 Wharton, G. Flood estimation from channel size: Guidelines for using the channel-geometry method. *Appl. Geogr.* **1992**, *12*, 339-359.
12 Wharton, G. The channel-geometry method: Guidelines and applications. *Earth Surf. Process. Landf.* **1995**, *20*, 649-660.
13 Bustamante, J.; Díaz-Delgado, R.; Aragonés, D. Determinación de las características de masas de agua someras en las marismas de Doñana mediante teledetección. *Revista de Teledetección* **2005**, *24*, 107-111.
14 Chow, V.T.; Maidment, D.R.; Mays, L.W. *Hidrología aplicada*; McGraw-Hill: Madrid, Spain, 1994.
15 SCS (Soil Conservation Service). *National Engineering Handbook*; Section 4, U.S. Department of Agriculture: Washington, DC, USA, 1972.
16 SCS (Soil Conservation Service). Hydrology. In *National Engineering Handbook*; Section 4; U.S. Department of Agriculture: Washington, DC, USA, 1985.
17 Solís, L. Hidrología, 2005. Available online: http://212.81.159.185:8080/hidrologia/index.html (accessed on 10 September 2009).
18 Nanía, L.S.; Gómez Valentín, M. *Ingeniería Hidrológica*, Segunda Edición; Grupo Editorial Universitario, Granada, Spain, 2006; p. 280.
19 Témez, J.R. *Cálculo hidrometeorológico de caudales máximos en pequeñas cuencas naturales*. Dirección General de Carreteras, MOPU, Madrid, Spain, 1987.
20 Ferrer, J. *Recomendaciones para el cálculo hidrometeorológico de avenidas*; CEDEX M-37; CEDEX: Madrid, Spain, 1993.
21 Singh, S.K. Transmuting synthetic unit hydrograph into gamma distribution. *J. Hydrol. Eng.* **2000**, *5*, 380-385.
22 Témez, J.R. Extended and Improved Rational Method: Version of the Highways Administration of Spain. In *Proceedings of XXIV Congress of IAHR*, Madrid, Spain, September 1991; Volume A, pp. 33-40.
23 MOPU. Norma 5,1-I.C. Instrucción de carreteras. Dirección General de Carreteras, MOPU: Madrid, Spain, 1990.

24 Benito, G.; Grodek, T.; Enzel, Y. The geomorphic and hydrologic impacts of the catastrophic failure of flood-control-dams during the 1996-Biescas flood (Central Pyrenees, Spain). *Zeitschrift für Geomorphologie* **1998**, *42*, 417-437.

25 Rico, M.; Benito, G. Estimación de caudales de crecida en pequeñas cuencas de montaña: Revisión metodológica y aplicación a la cuenca de Montardit (Pirineos Centrales, España). *Cuaternario & Geomorfología* **2002**, *16*, 127-138.

26 Benito, G.; Thorndycraft, V.R. Palaeoflood hydrology and its role in applied hydrological sciences. *J. Hydrol.* **2005**, *313*, 3-15.

27 Jarrett, R.D. Hydraulics of high-gradient streams. *J. Hydraul. Div. Am. Soc. Civ. Eng.* **1984**, *110*, 1519-1539.

28 Jarrett, R.D. *Determination of Roughness Coefficient for Streams in Colorado*; USGS Water Resources Investigations Report 85-4004; 1985.

29 Jarrett, R.D. Errors in slope-area computations of peak discharges in mountain streams. *J. Hydrol.* **1987**, *96*, 53-67.

30 Jarrett, R.D. Hydrologic and hydraulic research in mountain rivers. *Water Resour. Bull.* **1990**, *26*, 419-429.

31 Manning's n Information Table. In *HEC-RAS*, Version 3.1.1.; U.S. Army Corps of Engineers, Hydrologic Engineering Center: Davis, CA, USA, 2003.

32 Conesa-García, C.; García-Lorenzo, R.; López Bermúdez, F. Bed stability variations after check dam construction in torrential channels (South-East Spain). *Earth Process. Landf.* **2007**, *32*, 2165-2184.

33 Conesa-García, C. Les 'ramblas' du Sud-est Espagnol: systèmes hydromorphologiques en milieu méditerranéen sec. *Zeitschrift für Geomorphologie* **2005**, *49*, 205-224.